

## Title

Advances and opportunities in development of deformable organic electrochemical transistors

Brian V. Khau\*, Audrey D. Scholz\*, Elsa Reichmanis\*\*

\*denotes equal contribution

\*\*corresponding author: elr420@lehigh.edu<sup>1</sup>

Brian V. Khau, Elsa Reichmanis

School of Chemical & Biomolecular Engineering, Georgia Institute of Technology, Atlanta, Georgia 30332-0100, United States

Audrey D. Scholz, Elsa Reichmanis

School of Chemistry & Biochemistry, Georgia Institute of Technology, Atlanta, Georgia 30332-0100, United States

Keywords: organic electrochemical transistor, bioelectronics, deformability, PEDOT:PSS

## ORCID

Brian V. Khau: 0000-0003-4971-8366

Audrey D. Scholz: 0000-0003-2313-3706

Elsa Reichmanis: 0000-0002-8205-8016

## Abstract

Organic electrochemical transistors (OECTs) have arisen as potentially versatile platforms for bioelectronic applications due to their high transconductance, direct ionic-electronic coupling, and unique form factors. This perceived applicability to bioelectronics can be attributed to the incorporation of organic mixed conductors that facilitate both ionic and electronic transport, enabling material-inherent translation from biological signals to abiotic readouts. The past decade has yielded synthetic design principles to expand the limited materials space, yet unified guidelines for development of deformable OECTs for bioelectronics remains unclear. In this Perspective, we highlight recent advancements for imparting deformability. Specifically, materials selection, design, and chemistry for integral parts of the transistor – substrate, electrolyte, interconnects, and (polymeric) channel materials —will be discussed in the context of benchmarks set by bioelectronics applications. Additionally, we also identify key areas for future research and development of mechanically compliant OECTs.

---

<sup>1</sup> **Current address:** Elsa Reichmanis, Department of Chemical and Biomolecular Engineering, Lehigh University, Bethlehem, PA 18015.

## 1. Introduction

In the past decade, the organic electrochemical transistor (OECT) has been revived as a fervently studied device architecture in organic bioelectronics, where organic semiconductors are considered as interpreters between biologically driven processes and electronic signals.<sup>1,2</sup> To date, the OECT has been utilized for a potpourri of healthcare applications, ranging from electrophysiological monitoring<sup>3-6</sup> to metabolite detection.<sup>7-10</sup> Compared to devices with inorganic semiconductors, OECTs provide several key advantages that make them suitable for adoption in biomedical devices. First, OECTs are amenable to low-temperature processing techniques such as inkjet or screen printing<sup>11</sup> because their channel materials are solution-processable. This property means that arrays of OECTs can be manufactured and monolithically integrated on deformable substrates with low thermal budgets, such as polyethylene terephthalate (PET).<sup>12</sup> Second, the organic nature of OECT channel materials mean that a large synthetic toolbox, adopted from tangent organic electronics fields, can be applied to tune both (opto)electronic and ionic properties to match the desired applications.<sup>13, 14</sup> Third, the OECT operates at voltages  $< 1\text{ V}$ <sup>15</sup>, making it compatible for measuring and stimulating the millivolt potentials often observed in biological processes. Because organic materials for OECTs provide strong ionic-electronic coupling<sup>16, 17</sup>, OECTs serve as active transducers that provide amplification at the measurement site, in contrast to passive electrodes which perform external signal processing and amplification.

The contemporary OECT is a type of transistor similar in form to an electrolyte-gated transistor, but without a dielectric layer. The channel is composed of an organic semiconductor with demonstrated ability to interact with both electrons/holes and ions (i.e. an organic mixed ionic-electronic conductor) and immersed in an electrolyte. As common to most transistor architectures, the OECT is a three-terminal device composed of source, drain, and gate electrodes. The source and drain electrodes flank the channel and yield electrical readings of the organic material; the gate electrode is separated from the source/drain electrodes and provides electrical contact to the electrolyte. In bioelectronic applications, the gate electrode can often be replaced or chained to an element to be sensed. Unlike other transistors, the OECT operates via electrochemical instead of field-effect (de)doping. In this process, charge carriers in the bulk of the organic semiconductor are faradaically generated and couple to counterions from the electrolyte,<sup>18</sup> modulating the conductivity of the channel. The difference in charge dimensionality makes OECTs exceptional amplifiers but limits their switching speed to time scales of ion-transport between the electrolyte and the semiconductor bulk. For instance, a carboxylated polythiophene exhibited turn-on times of  $< 10\text{ ms}$  in the field-effect regime, but 3.4 seconds in the electrochemical regime.<sup>19</sup> Thus, the OECT should not be naively considered as a high-performing panacea, especially in areas such as transistor-based biosensors<sup>20</sup>, but as an emergent device architecture whose inherent three-dimensional charge transport and low-voltage operation lends itself to potentially exciting biological applications.

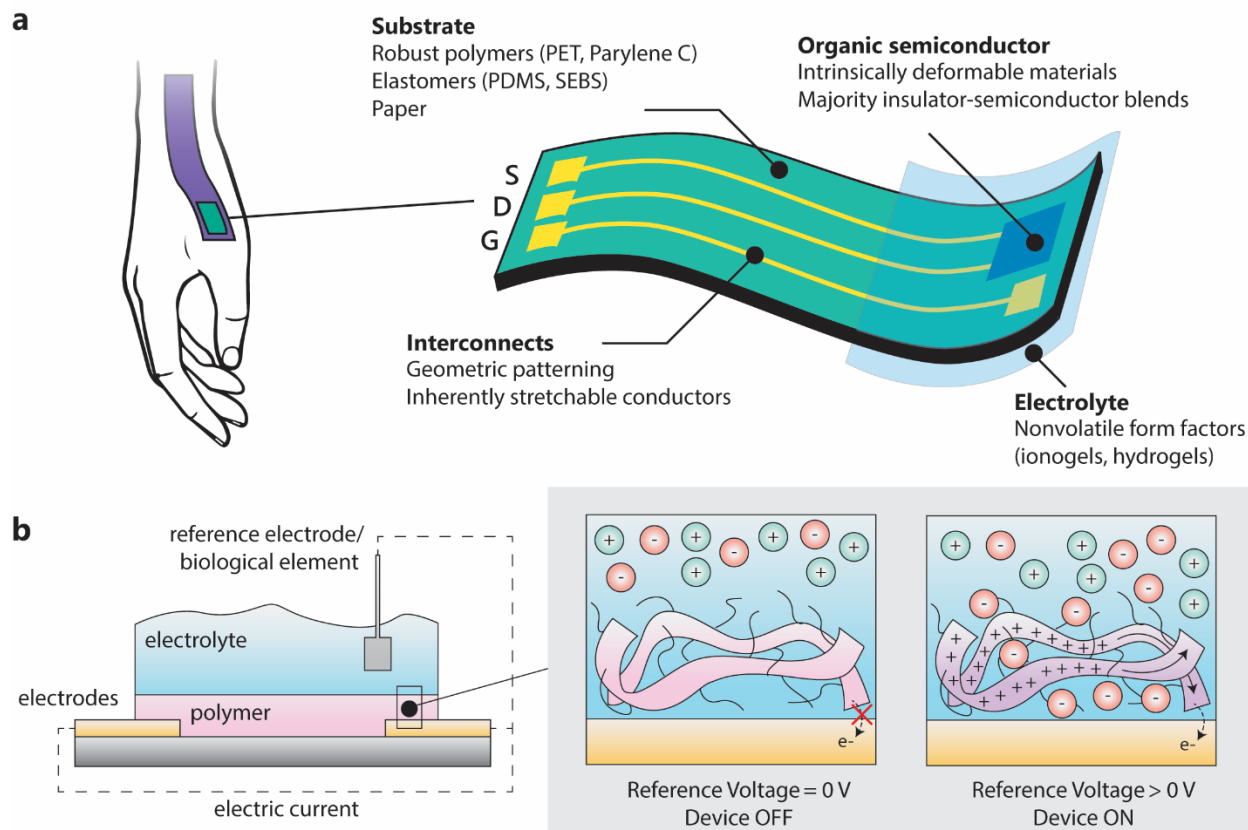


**Figure 1.** (a) Scheme of deformable OEET, visualized as an *ex vivo* skin-based sensor. (b) Side view of an OEET at the polymer-electrode interface, with associated polymer changes during electrochemical doping for a prototypical p-channel, accumulation-mode (or enhancement-mode) material.

This Perspective starts with a general discussion of several key material requirements for OEETs used in bioelectronics applications. Specifically, state-of-the-art innovations for imparting mechanical compliance will be discussed, along with their respective research gaps. Engineering methods and their associated impacts to incorporate flexibility and stretchability into the different parts of the transistor – substrate, electrolyte, contacts/interconnects, and channel material – will be discussed in detail. We will conclude with a summary of our personal views on critical challenges and proposed paths forward in this research space.

## 2. Mechanical Requirements for Deformable OEETs

Implicit in the discussion of OEETs as bioelectronic devices is the assumption that such devices can be fabricated in mechanically compliant form factors. We use “deformability” to broadly refer to properties that endow mechanical compliance. To precisely define vague concepts like flexibility and stretchability, we refer to a review on mechanical properties in pi-conjugated materials<sup>21</sup>, where flexibility is used to refer to devices that can be bent to curvature with radii < 1 cm, and stretchability to refer to devices that can undergo >5% elongation (where the deformation is plastic or elastic). Elongation here refers to the differential change in length over the initial length (i.e.  $\epsilon = \Delta L/L_0$ , also known as engineering strain), but we note that this begins to differ significantly from the true instantaneous strain  $e = \ln(1 + \epsilon)$  at engineering strains of 10%.

Regardless, the bioelectronics literature overwhelmingly uses the engineering strain for quantifying stretchability. Hereby, strain in this Perspective refers specifically to engineering strain.

Depending on application, the mechanical requirements for integration and interfacing vary greatly. For wearable sensors, deformable OECTs must be able to maintain a baseline of mechanical imperceptibility (i.e. a low tensile modulus consistent with skin, 60-70 MPa) and elongations of 60-75%, when skin reaches its maximum extensibility prior to fracture.<sup>22</sup> These elongation values can be relaxed depending on the location of the sensor; values measured on the wrist range from 11-23%.<sup>23</sup> For neural interfacing, substrates or encapsulation must match moduli of brain tissue on the order of 2 kPa,<sup>24</sup> which is a requirement met by few materials (e.g. hydrogels). For OECTs integrated into surface electrodes, the need for stretchability can be reduced significantly, as these devices monitor relatively static biological systems compared to external sensors.

The predominant form factor for mechanically compliant OECTs comprise planar architectures with poly(3,4-ethylenedioxythiophene)-poly(styrenesulfonate) (PEDOT:PSS) as the channel material, patterned on polymeric or elastomeric substrates. The predominance of PEDOT:PSS over other channel materials in the current literature is not unexpected; PEDOT:PSS has widely been used for applications ranging from actuators to transparent electrodes in organic devices. It is also commercially accessible in formulations of different viscosity for a myriad of coating and printing processes. Recent progress in deformable OECTs can be summarized below—the channel materials for these devices are PEDOT:PSS blended with plasticizers, conductivity enhancers, and/or crosslinkers unless explicitly stated otherwise.

**Table 2.** Representative architectures used to fabricate deformable OECTs. Not all works incorporating deformable OECTs are listed here.

Substrate	Electrolyte	Interconnects	Mechanical Properties/ Other notes	Ref.
Coated paper	PBS (aq)	PEDOT:PSS	Deformability not tested; inkjet printing combined with bio-immobilization (PEDOT:PSS blended with enzyme and mediator)	25
PET	PBS (aq)	Ti/Pt	Robust 1000 times bending at 5% strain	26
PDMS	PBS (aq)	Cr/Au with sequential PEDOT:PSS coat	30% biaxial strain resulted in 75% retention of drain current; PDMS was also templated (topology modification)	27
PDMS	NaCl (aq)	Microcracked Au	Up to 140% strain prior to high Au resistance; maintenance of transconductance at strains > 50%	28
PDMS	Hydrogel + NaCl	Cr/Au	Up to 30% biaxial strain before cracking; pre-straining strategy	29
Parylene C	Glycerol-based gel	Au	Unchanged operation at 30% strain; 98% retention of drain current after 1000 cycles of 20% strain	30

### 3. Interplay between device architecture and exhibited deformability

Because OECTs follow similar structures to organic field-effect transistors (OFET), many of the architectural concepts for introducing flexibility and stretchability are immediately translatable. Such concepts include strategies for off-loading the uniaxial, biaxial, or radial strains in a deformable device away from organic semiconductors. These innovations have been extensively researched since the late 1990s; we refer the reader to extensive works by Wagner, Suo, Rogers, and Someya.<sup>31-36</sup> These strategies have emerged because the materials characteristics needed for charge transport, such as rigid pi-conjugated polymer backbones<sup>37</sup> and high degrees of aggregation in the condensed state<sup>38</sup> often produce brittle organic semiconductors.<sup>21</sup> This subsection will be

broken down into strategies that implement deformability without using intrinsically deformable semiconductors.

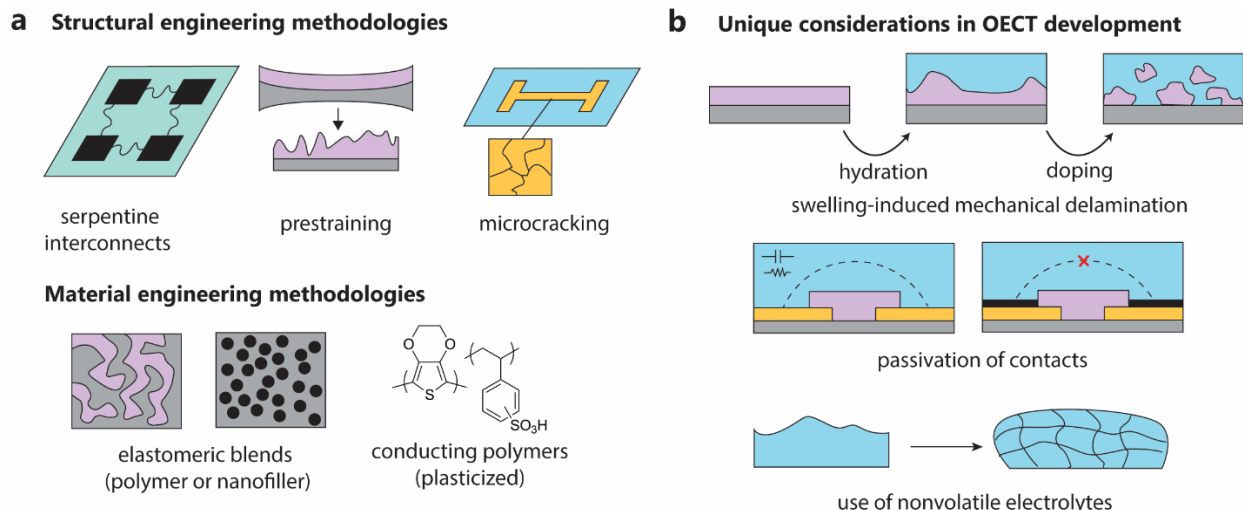


**Figure 2.** (a) Summary of structural and material engineering methodologies used in deformable electronics. (b) Schemes demonstrating architectural challenges that must be met when designing deformable OECTs that extend beyond standard paradigms used in OFETs.

### 3.1 Substrate Selection

As a bioelectronic device, the OECT presents a unique challenge that constrains the number of viable substrate materials. Film adhesion between the substrate and organic semiconductor is especially problematic in OECTs; organic films contract during deposition/annealing and swell significantly with electrolyte during operation. For instance, in a series of glycolated polythiophenes, p(g6T2-T) exhibited partial delamination and dispersion during stability testing due to its long glycolated side chains.<sup>39</sup> This problem is prevalent in conducting polymers used in wet, physiologically relevant environments; weak polymer-substrate adhesion in PEDOT:PSS, polypyrrole, and polyaniline result in debonding during operation.<sup>40-42</sup> Current substrate selection in OECTs does not consider strategies for reducing mechanical failure, including surface topology modification (e.g. roughening of substrates<sup>43</sup>) or coating of an interlayer<sup>44</sup> to promote adhesion.

The most frequently used polymeric substrates for flexible OECTs are polyethylene terephthalate (PET)<sup>12, 45-49</sup>, polyethylene naphthalate (PEN)<sup>50</sup>, and parylene C.<sup>51, 52</sup> Both PET and PEN possess several attractive properties, including optical transparency, low cost, and nm-level surface roughness when planarized.<sup>53</sup> However, both polyethylene derivatives are limited to processes with low thermal budgets. They are not compatible with manufacturing processes like reflow soldering or annealing that operate above the polymers' thermal decomposition temperatures. Parylene C is another inert polymer that has been widely used in bio-interfaces, as it exhibits biocompatibility and biostability.<sup>54, 55</sup> Unlike PET and PEN, it must be vapor processed—consequently, extremely thin layers of parylene C can be achieved, but it is not compatible for roll-to-roll processing. These polymers are not conductive to high degrees of biaxial strain.

For high levels of stretchability, elastomers such as polydimethylsiloxane (PDMS)<sup>29, 49, 56-59</sup> and styrene-ethylene-butadiene (SEBS)<sup>60, 61</sup> are used instead. PDMS is a popular elastomer for microfabrication as it can be easily patterned, provides biocompatibility, and exhibits softness

comparable to skin. Its hydrophobicity can prevent many inks from adhering to its surface, so primers, bonding layers, or oxygen plasma exposure are used to condition the PDMS surface prior to feature deposition. Another potential substrate that has not been used for OECT fabrication is polyurethane (PU), which is one of the most popular and versatile elastomers for other biomedical applications.

Paper can be used for fabrication of flexible OECTs, especially for *ex vivo* applications. The substrates used in reports of paper-based OECTs<sup>15, 25, 62, 63</sup>, have been coated papers. Compared to office and wove paper, coated papers demonstrate decreased roughness ( $\sim 10$  nm)<sup>64</sup>, providing a smooth surface for inkjet printing of prototype devices. Although these other paper types have not been used, cellulose-based papers as a whole provide intriguing opportunities for functionalization, as demonstrated by paper-based “lab-on-a-chip” devices popularized by the Whitesides group. Although the cellulose-based matrix that composes these papers is insulating, their porous structure endows them with high surface area, facilitated immobilization of active materials, and resistance to delamination of organic films.

### 3.2 Interconnects / Contacts

To provide electrical contact from the active channel to external measurables or data readouts, contacts and interconnects are required in any device. In an OECT, the proximity of the ionic electrolyte to these features adds an additional layer of complexity. Passivation between the interconnects and the electrolyte are required to prevent interactions occurring at the interconnects and/or minimize parasitic capacitance effects. In addition to high electrical conductivity, these passivated interconnects should be electrochemically stable at the operating windows of the device to preclude side reactions or decomposition from occurring.

In terms of technological difficulty, flexibility in interconnects is easier to achieve than stretchability. Many flexible devices utilize metallic interconnects, as hard metals and silicon can be made flexible when sufficiently thinned.<sup>32</sup> These contacts are thermally evaporated on the substrate with the help of intermediate adhesion layers, so that the interconnects are composed of Cr/Au<sup>3</sup> and Ti/Pt.<sup>46</sup> If printing is desired, printable conducting formulations are available, including silver-based paints<sup>12</sup> and PEDOT:PSS<sup>25</sup> utilized for many organic electronic devices. One must take care to separate these contacts from the electrolyte, especially as PEDOT:PSS is itself an active material for OECTs. In this case, care must be taken to passivate the conducting polymer from the electrolyte using impermeable materials such as parylene.

Development of stretchable interconnects can be divided into two categories: structural and material-based, although these two categories are not mutually exclusive. Structural-based interconnects rely on patterning of metals and other “hard” materials into certain shapes to reduce deformation in the active material.<sup>31, 36</sup> While this enables the use of rigid components, structure-based methods like serpentine structures reduce the area available to pattern devices. Material-based interconnects rely on use of inherently stretchable materials. Because most elastomeric materials are insulating, they are usually blended with an electrically conductive component to function as interconnects.<sup>65, 66</sup>

Key strategies of structural engineering for stretchability include serpentine structures, microcracking, and prestretching. Serpentine shapes act like closed springs and achieve strains of

around 30% through extension<sup>67</sup>. While straightforward to fabricate, serpentine structures exhibit tradeoffs between flexibility and in-plane stretchability. Microcracking is another strategy implemented when metallic species, such as Au, are thermally evaporated onto a weakly adhering substrate, such as PDMS. When strained, the Au film spontaneously undergoes microcracking, with non-negligible conductivities even when strained >100%. This strategy has been successfully to fabricate PEDOT:PSS-based OECTs with unprecedented transconductances at >50% strain.<sup>59</sup> Because Au is not inherently stretchable, experimental optimization is required to reduce and control strain-induced crack propagation. Prestretching can be used to “prestrain” a film. In this strategy, the interconnects are fabricated on a prestrained elastomeric film. When the film is released, longitudinal wave structures spontaneously form, enabling stretchability.<sup>68</sup> This method results in large out-of-plane bending strain to the material and can result in mechanical failure, so care must be taken to minimize bonding adhesion between the film and elastomer. This method has also been successfully to fabricate OECTs that have nearly unchanged electrical responses at 30% strain.<sup>29</sup>

Inherently stretchable materials can also be used to compose interconnects, including liquid metals<sup>69, 70</sup>, conducting polymers<sup>71</sup>, and elastomer-conducting filler composites.<sup>72</sup> Although liquid metals such as eutectic gallium-indium alloy (EgaIn) are prominently used for stretchable organic electronics applications, their high electrochemical reactivity<sup>70</sup> precludes their use in OECTs. Thus, we will primarily highlight conducting polymers and elastomers as forward-looking materials for interconnects.

As aforementioned, PEDOT:PSS can be used for flexible interconnects if it is well-passivated to prevent ionic conduction. This can be achieved by coating of a passivation layer between the electrolyte and the contact lines, such that the interconnects are still electrically connected to the channel. For stretchable OECTs, PEDOT:PSS must be plasticized with additives such as glycerol<sup>29</sup> or low molecular weight polyethylene glycol<sup>57</sup>, or blended with high molecular weight soft polymers<sup>73</sup> like polyethylene oxide (PEO) or polyvinyl alcohol (PVA). Such strategies can increase PEDOT:PSS’s elongation at break from 2% to over 50%.<sup>73</sup> Alternatively, elastomers with conductive fillers may be substituted for metal interconnects, where conductivity is traded for stretchability, yielding maximum strain values unreachable via structural strategies. For instance, Ag nanowires embedded in a polyurethane (PU) matrix<sup>72</sup> enable maximum strain values > 150% and could be used in future OECT works.

### 3.3 Electrolyte

The electrolyte of an OECT is one of its fundamental parts, providing a source of counterions, hydrating the organic film, and enabling large areal capacitances. Yet, much of the research focus in the OECT field has focused on generating channel materials that offer mixed conduction, instead of examining new paradigms for electrolytes. Most fundamental materials studies utilize 0.1 M NaCl (*aq*) or 1X PBS as the test electrolyte. While these studies are necessary and applicable to OECTs in hydrated environments, development of nonvolatile electrolytes is an equally important goal for future integration of OECTs into both *in vivo* and *ex vivo* applications.

The key characteristics for an ideal (semi-)solid electrolyte for OECTs are high ionic conductivity to reduce the polarization time of the OECT, electrochemical stability, and mechanical robustness for the desired application. Additionally, electrolytes should be developed with bio-interfacing and integration in mind and consequently should not be composed of cytotoxic materials. Stretchable

OECTs require electrolytes that can withstand a significant amount of elongation % before break, while electrolytes for flexible OECTs have no such requirement. To date, nonvolatile electrolytes for OECTs have followed numerous strategies, including (1) increasing viscosity by incorporating ionic liquids<sup>74</sup>, or utilization of binary mixtures of aqueous electrolytes with gelators/ionic liquids<sup>75</sup>, (2) cross-linking of ionic liquids into a polymeric matrix to form ionogels<sup>76, 77</sup>, and (3) hydrogels.<sup>29, 78, 79</sup> For noncytotoxic applications, use of mechanically robust ionogels or hydrogels are required.

Ionogels are composed of room-temperature ionic liquids (RTILs) mixed with gelators, which yield solid or gel-like polymeric materials. As a hybrid material, ionogels combine defined dimensional structure with the advantages of RTILs, including large electrochemically stable windows and high ionic conductivity. An additional advantage imparted by RTILs is that proteins and other biomolecules can be readily solubilized for long shelf-life (up to 18 months).<sup>80</sup> Thus, ionogels can be utilized to immobilize enzymes and mediators for targeted detection of bioanalytes. Early OECTs utilizing ionogels as the electrolyte have been used for detection of lactate<sup>76</sup> and glucose<sup>77</sup>, although these works do not touch on mechanical properties. Because ionogels are composed of RTILs, care must be taken to utilize ionic species that are innocuous if ionogels are to be utilized in direct contact with tissue.

As a potentially biocompatible alternative, hydrogels can be viably used as electrolytes for OECTs due to their significant water content. While compatible with extremely soft materials, cited hydrogels for OECTs may lack mechanical robustness needed for significant stretchability. For example, utilization of a 83 w/w% water polyethylene glycol-based hydrogel for OECTs was only stressed at strains of 0.4%.<sup>78</sup> Zhang et al. utilized a stretchable polyacrylamide “cut and paste” hydrogel in developing stretchable OECTs utilizing PEDOT:PSS, which yielded stable operation at 30% strain.<sup>29</sup> Failure beyond this was due to cracking of the PEDOT:PSS layer but not the hydrogel.

While hydrogels are excellent intermediaries for short-term operation, the evaporation of water can pose issues for long-term stability, especially for device architectures not conducive to evaporation. Glycerol-based gels are an excellent alternative to hydrogels, as glycerol is a biocompatible, nonvolatile liquid with a boiling point of 290 °C. Use of ultra-thin glycerol-based gels in compliant OECTs enabled measurement of high-fidelity electrocardiograms from skin without the need for an external electrolyte and demonstrated only a 2% decrease of drain current after 1000 strain cycles repeated at 0 - 20% strain.<sup>30</sup>

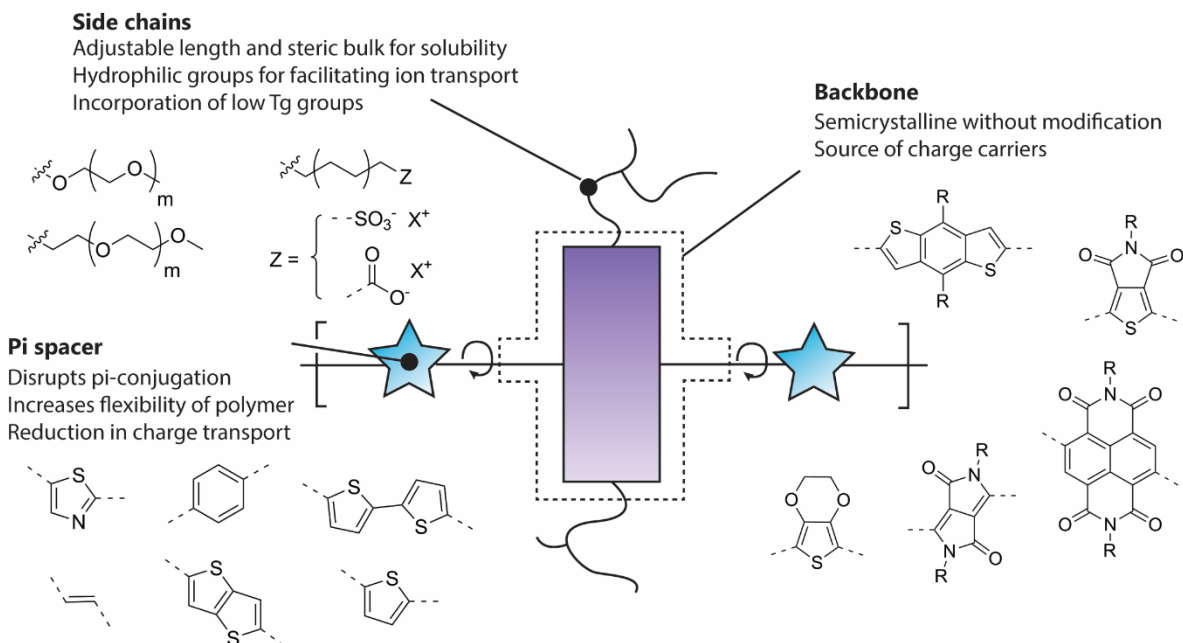
#### **4 Towards intrinsically deformable channel materials**

In addition to the above recommendations, deformable devices can utilize simpler architectures if all components, including the channel are intrinsically deformable. While the requirements of organic mixed ionic-electronic conductors – high degrees of charge transport and ionic facilitation – constrict the number of available options for designing new materials, numerous advances in the OFET area for stretchable and self-healing applications may be utilized for OECTs. This Perspective will focus primarily on polymeric systems used in OECTs, as their high molecular weights lead to entanglements that reportedly enable increased strength and toughness. While small-molecule semiconductors likely consume less energy to fracture or deform compared to their



polymeric counterparts<sup>81</sup>, this discrepancy may not matter when the film is encapsulated; nearly all of the energy required to deform the device is provided by the substrate.

### a Synthetic Design



### b Post-polymerization Methods

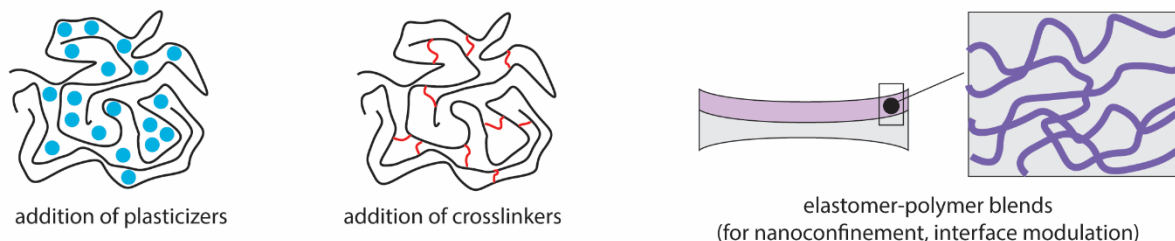


**Figure 3.** (a) Summary of potential synthetic design strategies for designing intrinsically deformable (polymeric) semiconductors. (b) Visualization of post-polymerization strategies.

### 4.1 State-of-the-Art Synthetic Design

PEDOT:PSS has been widely used as the *de facto* material in OECTs, both for investigation of processing techniques<sup>82, 83</sup>, as well as adoption in nearly all deformable OECTs to date. This popularity can be attributed to the commercial availability of PEDOT:PSS, demonstrated mixed conduction performance in OECTs<sup>84</sup>, and amenability to blending approaches to modify mechanical properties.<sup>85</sup> However, the nature of PEDOT:PSS as a mixture of two ionomers obfuscates attempts to derive structure-property interrelationships in polymers appropriate for OECTs. Additionally, the self-doping nature of PEDOT:PSS means that it forms devices that are nominally ON when no bias is applied (depletion-mode), which drove the need for accumulation-mode materials that are inherently insulating at neutral voltage bias.

The contemporary formula for design of mixed conductors involves the union of a high-charge transporting backbone (e.g. polythiophene, benzodithiophene, naphthalene-1,4,5,8-tetracarboxylic

diimide) known from the organic electronics literature, with an ionically functional side chain, of which the most popular are the oligoether side chains. We refer the reader to comprehensive materials reviews for more in-depth discussion regarding material design strategies.<sup>14</sup> Initial attempts at probing the impact of backbone planarity and varying degrees of triethylene glycol (TEG) sidechain density focused on utilization of different copolymers of thiophene, bithiophene, and benzodithiophene.<sup>86</sup> While this study and many others provided preliminary insight towards developing high-performance OECT materials, little attention has been paid to relating synthetic efforts to mechanical properties.

## 4.2 Engineering flexibility into OECT-type materials

*Synthetic Modifications.* Substitution of the alkyl side chains typically found in these polymers for oligoether and other hydrophilic side chains can have a dramatic impact on thermomechanical properties and condensed-state packing. The oligoether side chain seen in OECT materials grant polymers with increased hydrophilicity, a depressed glass transition from more flexible side chains, and improved ion-conductive behavior.<sup>88</sup> For example, in a series of polymers with a donor-acceptor backbone of *N*-substituted diketopyrrolopyrrole (DPP) and thiophene, the crack-onset strain increases as the side chain is changed from linear alkyl, oligoether, and branched alkyl chains, although the variance in molecular weight means it is hard to draw definitive conclusions.<sup>89</sup>

Conjugated pi-spacers along the polymer backbone can also be a useful tool to reduce the rigidity of individual polymer chains by creating a potential point of rotation (**Figure 3**)<sup>90-95</sup>. Sun et al. used a stiff ladder polymer benzimidazobenzophenanthroline (BBL) as the active material in an OECT but found the ion permeation rate to be an issue<sup>96</sup>. The backbone rigidity contributed to a high electron mobility, but the lack of hydrophilic side chains limited the ion permeation. On the other hand, Giovannitti et al. demonstrated poor electron mobility as the limiting factor for transconductance in a bithiophene naphthalene diimide (NDI) based polymer<sup>97</sup>. The bithiophene unit creates points of rotation and flexibility through the polymer, but the push-pull characteristic of the donor-acceptor polymer likely resulted in charge trapping. An all-acceptor backbone could be the answer to increasing the electron mobility while maintaining backbone flexibility in n-channel OECTs. As a pointed note, we caution that against assuming that backbone flexibility results in mechanically compliant films; backbone flexibility dictates the mechanical properties of isolated polymer chains, but solid-state packing and microstructure likely dictates the mechanical properties in as-cast thin films.<sup>21</sup>

*Post-polymerization Modifications.* Blends of materials with different mechanical and electrical characteristics have often been shown extensively to achieve a synergistic relationship. For instance, the combination of a high performing, brittle poly(dihexadecyl-cyclopentadithiophenyl)thiadiazolo-pyridine (PCDTPT) semiconductor with a malleable semiconductor poly(3-hexylthiophene) (P3HT) resulted in a highly flexible material, without significantly sacrificing charge transport<sup>98</sup>. This was rationalized because of small segments of ordered, rigid polymer in the vertical phase, enabling access to the dielectric layer. Our group also has success in utilizing extensive blending approaches for fabrication of highly flexible OFETs. Chu et al. combined the more mechanically compliant regiorandom P3HT with regioregular P3HT to

produce flexible OECTs with improved charge-carrier mobility and flexibility than pristine regioregular P3HT transistors.<sup>99</sup>

Semiconductors can blend with insulating elastomers such as P3HT and SEBS to simultaneously increase their charge-transport performance and mechanical compatibility. These seeming conflicting phenomena are potentially explained by the effects of nanoconfinement, where polymers' properties and crystallization can be significantly altered. For instance, the mechanical modulus and glass transition can decrease as compared to solution-processed films; growth of large crystallites is also restricted.<sup>100</sup> Our group combined the ductile insulator PDMS with three different semiconducting polymers to generate successful charge transport with as little as 0.5 wt% semiconductor<sup>101, 102</sup>. In this case, the phase-separating propensity of the disparate materials lead to interpenetrating networks which could withstand up to 100% stretchability. Polystyrene-block-poly(ethylene-butylene)-block-polystyrene (SEBS) is another elastomer that has been combined with a DPP-based semiconducting polymer to integrate the stretchability of the insulator with the charge transport capabilities of the semiconductor<sup>100</sup>. The resulting material withstood 100% strain with no diminishment in charge transport and was successfully integrated into a wearable electronic device. It is important to clarify that improved stretchability was achieved by reducing the film thickness, a common approach to achieving stretchability of conducting polymers<sup>103</sup> but problematic considering OECT performance relies on the volume of active material. The prototypical OECT material, PEDOT:PSS, can also be blended with a commercially available polyurethane to yield ~700% strain at fracture.<sup>104</sup> While promising, application of this strategy to some OECT materials may potentially be a difficult endeavor, due to the highly nonpolar character of elastomers and the polar side chains of OECT materials.

Cross-linkers, plasticizing additives, and conductivity enhancers can also be used to significantly modify the mechanical and electronic properties of active materials. In nearly all the cited deformable OECTs, the PEDOT:PSS was deposited with small percentages of additives, such as glycerol for conductivity enhancement and cross-linkers such as (3-glycidyloxypropyl)trimethoxysilane (GOPS) to yield water-insoluble films with significant mixed conduction behavior. As applied to OECTs, Cicoira and coworkers utilized the elastomeric properties of low molecular weight polyethylene glycol (PEG) to induce stretchability in PEDOT:PSS OECTs by minimizing the formation of cracks under strain<sup>105</sup>. We recommend that the reader should examine works related to electroactive actuators in the field, as these provide relevant information on incorporating stretchability into conductive polymers like PEDOT:PSS. These examples, and the aforementioned blending examples, demonstrate the power of post-processing to manipulate the mechanical properties of organic semiconductors towards mechanical compliance.

## 5. Conclusions and Outlook

In this Perspective, we have discussed key trends and challenges in the emerging area of deformable OECTs, breaking the OECT down into four critical components: the substrate, interconnects, electrolyte, and active material. As a transistor, the OECT shares many commonalities with other organic electronics devices, such that a researcher to the field can utilize pre-existing deformability paradigms. While the field has actively prioritized new and high-performing mixed conduction materials, multiple fundamental questions essential for deformable

OECT design persist. We leave the reader with five research gaps that would significantly move the field forward.

*Design of (Semi-solid) Electrolytes.* As aforementioned, additional investigations are essential to develop semi-solid electrolytes for OECTs. Because these electrolytes typically consist of ionic components dispersed in a cross-linked polymeric matrix, their ionic conductivity is much lower than that of aqueous solution. The resulting long polarization time is detrimental to the switching speed of the device. Biocompatibility is essential for many of these applications, especially as key applications utilizing these transistors (e.g. ion pumps for drug delivery, neural interfacing, *ex situ* sensing) require direct contact with tissue. Glycerol-based gels by Someya and coworkers<sup>30</sup> appear the most promising, demonstrating little or no evaporation after 10 hours and long-term operation when tested with 20% strain. Additional mechanical studies corroborating this work and incorporating this gel on high-performance OECT materials besides PEDOT:PSS would be especially instructive.

*Electromechanical properties of polymeric mixed conductors.* While significant work has been conducted on tying together the emergent mechanical properties in conjugated polymers, a major research gap lies in determining how optoelectronic (and ionic) properties fundamentally evolve under strain. Studies examining the electromechanical properties in OFETs have largely been empirical. Consequently, it is difficult to generate or conceive of design motifs for synthesizing materials that are robust under deformation. A baseline model<sup>106</sup> to predict the electro-mechanical behavior in OFETs and OECTs combines the gradual-channel approximation with assumptions of isotropic incompressibility, although the authors note that no truly semiconducting polymers currently exist. In an OECT, these electromechanical models could be improved by incorporating the heterogenous effect of swelling and utilizing more complex charge models.

*Interrogation of molecular weight-dependent properties.* The majority of the glycolated polymers presently synthesized have reported molecular weights  $< 15 - 20$  kg/mol,<sup>14</sup> resulting in low degrees of polymerization. These are likely a result of the difficulty in the synthesis and purification of the hygroscopic polymers. Consequently, studies quantifying the impact of molecular weight on the  $T_g$  and microstructure have not been reported for OECT materials. In the prototypical poly(3-hexylthiophene) (P3HT), a “classic” semiconducting polymer, increasing molecular weight in melt-processed films resulted in a transition from brittle tensile behavior at 20 kg/mol (elongation at break =  $\sim 30\%$ ) to plastic deformation behavior at 110 kg/mol (elongation at break =  $\sim 300\%$ ).<sup>107</sup> Completing an analogous study for a subset of organic mixed conductors would provide insight towards qualifying the evolution microstructure in OECT materials and determining the nature of amorphous and crystalline fractions present in the film.

*Characterization of the break-in transition.* Another existing knowledge gap in the field is understanding the electrolytic break-in transition, where direct observation via *in situ* studies would be highly beneficial. Currently, swelling of a glycolated polymer, p(g2T-TT) was examined using *in situ* Raman to quantify pi-pi stacking, as well as *ex situ* grazing incidence wide-angle x-ray scattering (GIWAXS) of as-cast and doped films. It was found that water uptake in these films was not uniform and favored amorphous regions; demonstrating that films with a higher fraction of crystalline regions are not necessarily better for OECT charge transport.<sup>108</sup> This trend was also consistent with crystallinity studies for another glycolated polythiophene.<sup>109</sup> Understanding how

the supporting electrolyte impacts the crystalline composition and structural inhomogeneity of the film through *in situ* GIWAXS<sup>110</sup> and grazing-incidence small angle x-ray scattering (GISAXS), respectively, would partially answer the question of material property evolution. Direct observation of the impact of ion transport in and out of these films was also probed via electrochemical strain microscopy<sup>111</sup>, where strain heterogeneity can be compared with area-dependent stiffness to understand how hydration and electrochemical doping impacts local mechanical properties.

*Expansion of the Side Chain Toolbox.* As an emerging field, OECTs are also limited when it comes to active material selection. Many, if not all, of the conformal OECTs in literature report PEDOT:PSS formulations as their active material, and many new emerging materials appropriate known high-mobility backbones from the OFET literature and attaching glycolated side chains. While endowing backbones with glycolated side chains is a widely demonstrated motif, additional side chain engineering should emphasize exploring alternative side chains with hydrophilic functional groups that facilitate ion transport without sacrificing electronic performance. As a brief example, one might consider use of hydrogen-bonding side chain motifs such as carboxylic acids,<sup>19, 112, 113</sup> ureas<sup>114</sup>, and ureidopyrimidones<sup>115</sup> to endow polymers with enhanced self-assembly through noncovalent interactions. It is important to also note that introduction of a small fraction (5-10%) of hydrogen-bonding side chains into polymers with alkyl chains have yielded polymers with self-healability.<sup>116</sup> Additionally, focused studies on side chain length, density, and placement should be completed for these alternative sidechains – we point out that two such studies have been recently published for glycolated side chains in 2020.<sup>39, 117</sup>

## Conflicts of Interest

The authors declare no competing financial interest.

## Acknowledgments

The authors would like to acknowledge support from the National Science Foundation Grant No. 1809495: Interplay of Molecular Structure and Solution Behavior in High Performance Conjugated Polymers, the Georgia Institute of Technology, and the Pete Silas Chair funds for support. A.D.S. also appreciates support associated with a Department of Education GAANN Fellowship (P200A180075).

## References

1. M. Berggren and A. Richter-Dahlfors, *Advanced Materials*, 2007, **19**, 3201-3213.
2. D. T. Simon, E. O. Gabrielsson, K. Tybrandt and M. Berggren, *Chem Rev*, 2016, **116**, 13009-13041.
3. A. Campana, T. Cramer, D. T. Simon, M. Berggren and F. Biscarini, *Advanced Materials*, 2014, **26**, 3874-3878.
4. D. Khodagholy, T. Doublet, P. Quilichini, M. Gurfinkel, P. Leleux, A. Ghestem, E. Ismailova, T. Herve, S. Sanaur, C. Bernard and G. G. Malliaras, *Nat Commun*, 2013, **4**, 1575.
5. C. Yao, C. Xie, P. Lin, F. Yan, P. Huang and I.-M. Hsing, *Advanced Materials*, 2013, **25**, 6575-6580.
6. Y. Kim, T. Lim, C.-H. Kim, C. S. Yeo, K. Seo, S.-M. Kim, J. Kim, S. Y. Park, S. Ju and M.-H. Yoon, *NPG Asia Materials*, 2018, **10**, 1086-1095.
7. G. Scheiblin, A. Aliane, X. Strakosas, V. F. Curto, R. Coppard, G. Marchand, R. M. Owens, P. Mailley and G. G. Malliaras, *MRS Communications*, 2015, **5**, 507-511.
8. X. Ji, H. Y. Lau, X. Ren, B. Peng, P. Zhai, S.-P. Feng and P. K. L. Chan, *Advanced Materials Technologies*, 2016, **1**, 1600042.

9. M. Braendlein, A.-M. Pappa, M. Ferro, A. Lopresti, C. Acquaviva, E. Mamessier, G. G. Malliaras and R. M. Owens, *Advanced Materials*, 2017, **29**, 1605744.
10. A. M. Pappa, D. Ohayon, A. Giovannitti, I. P. Maria, A. Savva, I. Uguz, J. Rivnay, I. McCulloch, R. M. Owens and S. Inal, *Science Advances*, 2018, **4**, eaat0911.
11. M. Zabihipour, R. Lassnig, J. Strandberg, M. Berggren, S. Fabiano, I. Engquist and P. Andersson Ersman, *npj Flexible Electronics*, 2020, **4**.
12. P. Andersson Ersman, R. Lassnig, J. Strandberg, D. Tu, V. Keshmiri, R. Forchheimer, S. Fabiano, G. Gustafsson and M. Berggren, *Nat Commun*, 2019, **10**, 5053.
13. A. Facchetti, *Chemistry of Materials*, 2011, **23**, 733-758.
14. M. Moser, J. F. Ponder, A. Wadsworth, A. Giovannitti and I. McCulloch, *Advanced Functional Materials*, 2019, **29**, 1807033.
15. D. Nilsson, M. Chen, T. Kugler, T. Remonen, M. Armgarth and M. Berggren, *Advanced Materials*, 2002, **14**, 51-54.
16. B. D. Paulsen, K. Tybrandt, E. Stavrinidou and J. Rivnay, *Nat Mater*, 2020, **19**, 13-26.
17. J. Chung, A. Khot, B. M. Savoie and B. W. Boudouris, *ACS Macro Letters*, 2020, **9**, 646-655.
18. L. Q. Flagg, C. G. Bischak, R. J. Quezada, J. W. Onorato, C. K. Luscombe and D. S. Ginger, *ACS Materials Letters*, 2020, **2**, 254-260.
19. A. Laiho, L. Herlogsson, R. Forchheimer, X. Crispin and M. Berggren, *Proc Natl Acad Sci U S A*, 2011, **108**, 15069-15073.
20. R. A. Picca, K. Manoli, E. Macchia, L. Sarcina, C. Di Franco, N. Cioffi, D. Blasi, R. Österbacka, F. Torricelli, G. Scamarcio and L. Torsi, *Advanced Functional Materials*, 2019, **30**.
21. S. E. Root, S. Savagatrup, A. D. Printz, D. Rodriguez and D. J. Lipomi, *Chem Rev*, 2017, **117**, 6467-6499.
22. C. Edwards and R. Marks, *Clinics in Dermatology*, 1995, **13**, 375-380.
23. N. Lu, C. Lu, S. Yang and J. Rogers, *Advanced Functional Materials*, 2012, **22**, 4044-4050.
24. S. Budday, R. Nay, R. de Rooij, P. Steinmann, T. Wyrobek, T. C. Ovaert and E. Kuhl, *J Mech Behav Biomed Mater*, 2015, **46**, 318-330.
25. E. Bihar, S. Wustoni, A. M. Pappa, K. N. Salama, D. Baran and S. Inal, *npj Flexible Electronics*, 2018, **2**.
26. C. Liao, C. Mak, M. Zhang, H. L. W. Chan and F. Yan, *Advanced Materials*, 2015, **27**, 676-681.
27. Y. Li, N. Wang, A. Yang, H. Ling and F. Yan, *Advanced Electronic Materials*, 2019, DOI: 10.1002/aelm.201900566, 1900566.
28. N. Matsuhisa, Y. Jiang, Z. Liu, G. Chen, C. Wan, Y. Kim, J. Kang, H. Tran, H. C. Wu, I. You, Z. Bao and X. Chen, *Advanced Electronic Materials*, 2019, **5**, 1900347.
29. S. Zhang, E. Hubis, G. Tomasello, G. Soliveri, P. Kumar and F. Cicoira, *Chemistry of Materials*, 2017, **29**, 3126-3132.
30. H. Lee, S. Lee, W. Lee, T. Yokota, K. Fukuda and T. Someya, *Advanced Functional Materials*, 2019, **29**, 1906982.
31. S. Wagner and S. Bauer, *MRS Bulletin*, 2012, **37**, 207-213.
32. Z. Suo, E. Y. Ma, H. Gleskova and S. Wagner, *Applied Physics Letters*, 1999, **74**, 1177-1179.
33. J. Jones, S. P. Lacour, S. Wagner and Z. G. Suo, *J Vac Sci Technol A*, 2004, **22**, 1723-1725.
34. S. P. Lacour, S. Wagner, Z. Huang and Z. Suo, *Applied Physics Letters*, 2003, **82**, 2404-2406.
35. H. Gleskova, I. C. Cheng, S. Wagner, J. C. Sturm and Z. Suo, *Solar Energy*, 2006, **80**, 687-693.
36. J. A. Rogers, T. Someya and Y. Huang, *Science*, 2010, **327**, 1603-1607.
37. S. Savagatrup, X. Zhao, E. Chan, J. Mei and D. J. Lipomi, *Macromol Rapid Commun*, 2016, **37**, 1623-1628.
38. B. O'Connor, E. P. Chan, C. Chan, B. R. Conrad, L. J. Richter, R. J. Kline, M. Heeney, I. McCulloch, C. L. Soles and D. M. DeLongchamp, *ACS Nano*, 2010, **4**, 7538-7544.

39. M. Moser, L. R. Savagian, A. Savva, M. Matta, J. F. Ponder, T. C. Hidalgo, D. Ohayon, R. Hallani, M. Reisjalali, A. Troisi, A. Wadsworth, J. R. Reynolds, S. Inal and I. McCulloch, *Chemistry of Materials*, 2020, **32**, 6618-6628.
40. R. A. Green, R. T. Hassarati, L. Bouchinet, C. S. Lee, G. L. Cheong, J. F. Yu, C. W. Dodds, G. J. Suaning, L. A. Poole-Warren and N. H. Lovell, *Biomaterials*, 2012, **33**, 5875-5886.
41. L. Ouyang, B. Wei, C. C. Kuo, S. Pathak, B. Farrell and D. C. Martin, *Sci Adv*, 2017, **3**, e1600448.
42. H. Yuk, T. Zhang, S. Lin, G. A. Parada and X. Zhao, *Nat Mater*, 2016, **15**, 190-196.
43. C. Bohler, F. Oberueber, S. Schlabach, T. Stieglitz and M. Asplund, *ACS Appl Mater Interfaces*, 2017, **9**, 189-197.
44. A. Inoue, H. Yuk, B. Lu and X. Zhao, *Sci Adv*, 2020, **6**, eaay5394.
45. P. Lin, X. Luo, I. M. Hsing and F. Yan, *Adv Mater*, 2011, **23**, 4035-4040.
46. C. Liao, C. Mak, M. Zhang, H. L. Chan and F. Yan, *Adv Mater*, 2015, **27**, 676-681.
47. F. Mariani, I. Gualandi, M. Tessarolo, B. Fraboni and E. Scavetta, *ACS Appl Mater Interfaces*, 2018, **10**, 22474-22484.
48. C. Yao, Q. Li, J. Guo, F. Yan and I. M. Hsing, *Adv Healthc Mater*, 2015, **4**, 528-533.
49. S. Zhang, E. Hubis, C. Girard, P. Kumar, J. Defranco and F. Cicoira, *Journal of Materials Chemistry C*, 2016, **4**, 1382-1385.
50. G. Scheiblin, R. Coppard, R. M. Owens, P. Mailley and G. G. Malliaras, *Advanced Materials Technologies*, 2017, **2**.
51. W. Lee, D. Kim, N. Matsuhisa, M. Nagase, M. Sekino, G. G. Malliaras, T. Yokota and T. Someya, *Proc Natl Acad Sci U S A*, 2017, **114**, 10554-10559.
52. H. Lee, S. Lee, W. Lee, T. Yokota, K. Fukuda and T. Someya, *Advanced Functional Materials*, 2019, **29**, 1906982.
53. W. A. MacDonald, M. K. Looney, D. MacKerron, R. Eveson, R. Adam, K. Hashimoto and K. Rakos, *Journal of the Society for Information Display*, 2007, **15**.
54. T. Y. Chang, V. G. Yadav, S. De Leo, A. Mohedas, B. Rajalingam, C. L. Chen, S. Selvarasah, M. R. Dokmeci and A. Khademhosseini, *Langmuir*, 2007, **23**, 11718-11725.
55. B. J. Kim and E. Meng, *Polymers for Advanced Technologies*, 2016, **27**, 564-576.
56. S. Zhang, Y. Li, G. Tomasello, M. Anthonisen, X. Li, M. Mazzeo, A. Genco, P. Grutter and F. Cicoira, *Advanced Electronic Materials*, 2019, **5**.
57. Y. Li, S. Zhang, X. Li, V. R. N. Unnava and F. Cicoira, *Flexible and Printed Electronics*, 2019, **4**.
58. B. Marchiori, R. Delattre, S. Hannah, S. Blayac and M. Ramuz, *Sci Rep*, 2018, **8**, 8477.
59. N. Matsuhisa, Y. Jiang, Z. Liu, G. Chen, C. Wan, Y. Kim, J. Kang, H. Tran, H. C. Wu, I. You, Z. Bao and X. Chen, *Advanced Electronic Materials*, 2019, **5**.
60. O. Parlak, S. T. Keene, A. Marais, V. F. Curto and A. Salleo, *Sci Adv*, 2018, **4**, eaar2904.
61. S. T. Keene, D. Fogarty, R. Cooke, C. D. Casadevall, A. Salleo and O. Parlak, *Adv Healthc Mater*, 2019, **8**, e1901321.
62. E. Bihar, Y. Deng, T. Miyake, M. Saadaoui, G. G. Malliaras and M. Rolandi, *Sci Rep*, 2016, **6**, 27582.
63. D. Nilsson, T. Kugler, P. O. Svensson and M. Berggren, *Sensor Actuat B-Chem*, 2002, **86**, 193-197.
64. Y. Zheng, Z. He, Y. Gao and J. Liu, *Scientific Reports*, 2013, **3**.
65. N. Matsuhisa, X. Chen, Z. Bao and T. Someya, *Chem Soc Rev*, 2019, **48**, 2946-2966.
66. H. L. Filiatrault, G. C. Porteous, R. S. Carmichael, G. J. Davidson and T. B. Carmichael, *Adv Mater*, 2012, **24**, 2673-2678.
67. D. H. Kim, N. Lu, R. Ma, Y. S. Kim, R. H. Kim, S. Wang, J. Wu, S. M. Won, H. Tao, A. Islam, K. J. Yu, T. I. Kim, R. Chowdhury, M. Ying, L. Xu, M. Li, H. J. Chung, H. Keum, M. McCormick, P. Liu, Y. W. Zhang, F. G. Omenetto, Y. Huang, T. Coleman and J. A. Rogers, *Science*, 2011, **333**, 838-843.

68. N. Bowden, S. Brittain, A. G. Evans, J. W. Hutchinson and G. M. Whitesides, *Nature*, 1998, **393**, 146-149.
69. H.-J. Kim, C. Son and B. Ziaie, *Applied Physics Letters*, 2008, **92**.
70. M. D. Dickey, *Adv Mater*, 2017, **29**.
71. Y. Wang, C. Zhu, R. Pfattner, H. Yan, L. Jin, S. Chen, F. Molina-Lopez, F. Lissel, J. Liu, N. I. Rabiah, Z. Chen, J. W. Chung, C. Linder, M. F. Toney, B. Murmann and Z. Bao, *Sci Adv*, 2017, **3**, e1602076.
72. W. Hu, X. Niu, R. Zhao and Q. Pei, *Applied Physics Letters*, 2013, **102**.
73. P. Li, K. Sun and J. Ouyang, *ACS Appl Mater Interfaces*, 2015, **7**, 18415-18423.
74. S. Y. Yang, F. Cicoira, R. Byrne, F. Benito-Lopez, D. Diamond, R. M. Owens and G. G. Malliaras, *Chemical Communications*, 2010, **46**, 7972-7974.
75. Z. Yi, G. Natale, P. Kumar, E. D. Mauro, M.-C. Heuzey, F. Soavi, I. I. Perepichka, S. K. Varshney, C. Santato and F. Cicoira, *Journal of Materials Chemistry C*, 2015, **3**, 6549-6553.
76. D. Khodagholy, V. F. Curto, K. J. Fraser, M. Gurfinkel, R. Byrne, D. Diamond, G. G. Malliaras, F. Benito-Lopez and R. M. Owens, *Journal of Materials Chemistry*, 2012, **22**, 4440.
77. S. Y. Yang, F. Cicoira, R. Byrne, F. Benito-Lopez, D. Diamond, R. M. Owens and G. G. Malliaras, *Chem Commun (Camb)*, 2010, **46**, 7972-7974.
78. I. Del Agua, L. Porcarelli, V. F. Curto, A. Sanchez-Sanchez, E. Ismailova, G. G. Malliaras and D. Mecerreyes, *J Mater Chem B*, 2018, **6**, 2901-2906.
79. Y. J. Jo, K. Y. Kwon, Z. U. Khan, X. Crispin and T. I. Kim, *ACS Appl Mater Interfaces*, 2018, **10**, 39083-39090.
80. K. Fujita, D. R. MacFarlane, M. Forsyth, M. Yoshizawa-Fujita, K. Murata, N. Nakamura and H. Ohno, *Biomacromolecules*, 2007, **8**, 2080-2086.
81. D. Rodriguez, S. Savagatrup, E. Valle, C. M. Proctor, C. McDowell, G. C. Bazan, T. Q. Nguyen and D. J. Lipomi, *ACS Appl Mater Interfaces*, 2016, **8**, 11649-11657.
82. S. Zhang, P. Kumar, A. S. Nouas, L. Fontaine, H. Tang and F. Cicoira, *APL Materials*, 2015, **3**.
83. L. V. Lingstedt, M. Ghittorelli, H. Lu, D. A. Koutsouras, T. Marszalek, F. Torricelli, N. I. Crăciun, P. Gkoupidenis and P. W. M. Blom, *Advanced Electronic Materials*, 2019, DOI: 10.1002/aelm.201800804.
84. J. Rivnay, S. Inal, B. A. Collins, M. Sessolo, E. Stavrinidou, X. Strakosas, C. Tassone, D. M. DeLongchamp and G. G. Malliaras, *Nat Commun*, 2016, **7**, 11287.
85. L. V. Kayser and D. J. Lipomi, *Adv Mater*, 2019, **31**, e1806133.
86. C. B. Nielsen, A. Giovannitti, D.-T. Sbircea, E. Bandiello, M. R. Niazi, D. A. Hanifi, M. Sessolo, A. Amassian, G. G. Malliaras, J. Rivnay and I. McCulloch, *Journal of the American Chemical Society*, 2016, **138**, 10252-10259.
87. A. H. Schroeder and F. B. Kaufman, *Journal of Electroanalytical Chemistry and Interfacial Electrochemistry*, 1980, **113**, 209-224.
88. B. Meng, J. Liu and L. Wang, *Polymer Chemistry*, 2020, **11**, 1261-1270.
89. F. Sugiyama, A. T. Kleinschmidt, L. V. Kayser, D. Rodriguez, M. Finn, 3rd, M. A. Alkhadra, J. M. Wan, J. Ramirez, A. S. Chiang, S. E. Root, S. Savagatrup and D. J. Lipomi, *Polym Chem*, 2018, **9**, 4354-4363.
90. S. Dey, *Small*, 2019, **15**, 1900134.
91. Y. Wang, T. Hasegawa, H. Matsumoto, T. Mori and T. Michinobu, 2016, DOI: 10.1002/adfm.201604608.
92. M. Goel, C. D. Heinrich, G. Krauss and M. Thelakkat, *Macromolecular Rapid Communications*, 2019, **40**, 1800915.
93. C. J. Mueller, E. Gann, C. R. Singh, M. Thelakkat and C. R. McNeill, 2016, **28**, 7088-7097.
94. R. Sheng, Q. Liu, W. Chen, M. Sun, H. Zheng, J. Ren and R. Yang, 2015, DOI: 10.1002/pola.28017, n/a-n/a.



95. J. L. Brédas, G. B. Street, B. Thémans and J. M. André, *The Journal of Chemical Physics*, 1985, **83**, 1323-1329.
96. H. Sun, M. Vagin, S. Wang, X. Crispin, R. Forchheimer, M. Berggren and S. Fabiano, *Advanced Materials*, 2018, **30**, 1704916.
97. A. Giovannitti, C. B. Nielsen, D.-T. Sbircea, S. Inal, M. Donahue, M. R. Niazi, D. A. Hanifi, A. Amassian, G. G. Malliaras, J. Rivnay and I. McCulloch, *Nature Communications*, 2016, **7**, 13066.
98. T. Sun, J. I. Scott, M. Wang, R. J. Kline, G. C. Bazan and B. T. O'Connor, *Advanced Electronic Materials*, 2017, **3**, 1600388.
99. P.-H. Chu, G. Wang, B. Fu, D. Choi, J. O. Park, M. Srinivasarao and E. Reichmanis, 2016, **2**, n/a-n/a.
100. J. Xu, S. Wang, G.-J. N. Wang, C. Zhu, S. Luo, L. Jin, X. Gu, S. Chen, V. R. Feig, J. W. F. To, S. Rondeau-Gagné, J. Park, B. C. Schroeder, C. Lu, J. Y. Oh, Y. Wang, Y.-H. Kim, H. Yan, R. Sinclair, D. Zhou, G. Xue, B. Murmann, C. Linder, W. Cai, J. B. H. Tok, J. W. Chung and Z. Bao, *Science*, 2017, **355**, 59-64.
101. G. Zhang, M. McBride, N. Persson, S. Lee, T. J. Dunn, M. F. Toney, Z. Yuan, Y.-H. Kwon, P.-H. Chu, B. Risteen and E. Reichmanis, *Chemistry of Materials*, 2017, **29**, 7645-7652.
102. G. Zhang, S. Lee, E. Gutiérrez-Meza, C. Buckley, M. McBride, D. A. Valverde-Chávez, Y. H. Kwon, V. Savikhin, H. Xiong, T. J. Dunn, M. F. Toney, Z. Yuan, C. Silva and E. Reichmanis, *Chemistry of Materials*, 2019, DOI: 10.1021/acs.chemmater.8b05224.
103. S. Zhang, Y. Li, G. Tomasello, M. Anthonisen, X. Li, M. Mazzeo, A. Genco, P. Grutter and F. Cicoira, *Advanced Electronic Materials*, 2019, **5**, 1900191.
104. P. J. Taroni, G. Santagiuliana, K. Wan, P. Calado, M. Qiu, H. Zhang, N. M. Pugno, M. Palma, N. Stingelin-Stutzman, M. Heeney, O. Fenwick, M. Baxendale and E. Bilotti, *Advanced Functional Materials*, 2018, **28**, 1704285.
105. Y. Li, S. Zhang, X. Li, V. R. N. Unnava and F. Cicoira, *Flexible and Printed Electronics*, 2019, **4**, 044004.
106. V. G. Reynolds, S. Oh, R. Xie and M. L. Chabiny, *Journal of Materials Chemistry C*, 2020, **8**, 9276-9285.
107. F. P. V. Koch, J. Rivnay, S. Foster, C. Müller, J. M. Downing, E. Buchaca-Domingo, P. Westacott, L. Yu, M. Yuan, M. Baklar, Z. Fei, C. Luscombe, M. A. McLachlan, M. Heeney, G. Rumbles, C. Silva, A. Salleo, J. Nelson, P. Smith and N. Stingelin, *Progress in Polymer Science*, 2013, **38**, 1978-1989.
108. A. Savva, C. Cendra, A. Giugni, B. Torre, J. Surgailis, D. Ohayon, A. Giovannitti, I. McCulloch, E. Di Fabrizio, A. Salleo, J. Rivnay and S. Inal, *Chemistry of Materials*, 2019, **31**, 927-937.
109. L. Q. Flagg, C. G. Bischak, J. W. Onorato, R. B. Rashid, C. K. Luscombe and D. S. Ginger, *Journal of the American Chemical Society*, 2019, **141**, 4345-4354.
110. B. D. Paulsen, R. Wu, Wu, C. Takacs, Takacs, H.-G. Steinrück, J. Strzalka, Q. Zhang, M. Toney and J. Rivnay, *ChemRxiv*, 2020, DOI: 10.26434/chemrxiv.12312299.v1.
111. R. Giridharagopal, L. Q. Flagg, J. S. Harrison, M. E. Ziffer, J. Onorato, C. K. Luscombe and D. S. Ginger, *Nature Materials*, 2017, **16**, 737-742.
112. B. V. Khau, L. R. Savagian, M. De Keersmaecker, M. A. Gonzalez and E. Reichmanis, *ACS Materials Letters*, 2019, **1**, 599-605.
113. H. Toss, C. Suspène, B. Piro, A. Yassar, X. Crispin, L. Kergoat, M.-C. Pham and M. Berggren, *Organic Electronics*, 2014, **15**, 2420-2427.
114. J. Yao, C. Yu, Z. Liu, H. Luo, Y. Yang, G. Zhang and D. Zhang, *Journal*, 2016, **138**, 173-185.
115. Y.-H. Lin, S. B. Darling, M. P. Nikiforov, J. Strzalka and R. Verduzco, *Macromolecules*, 2012, **45**, 6571-6579.
116. A. Gasperini, G.-J. N. Wang, F. Molina-Lopez, H.-C. Wu, J. Lopez, J. Xu, S. Luo, D. Zhou, G. Xue, J. B. H. Tok and Z. Bao, *Macromolecules*, 2019, **52**, 2476-2486.

117. A. Savva, R. Hallani, C. Cendra, J. Surgailis, T. C. Hidalgo, S. Wustoni, R. Sheelamanthula, X. Chen, M. Kirkus, A. Giovannitti, A. Salleo, I. McCulloch and S. Inal, *Advanced Functional Materials*, 2020, **30**, 1907657.